

Communication

Photooxidation of *p*-Arsanilic Acid in Aqueous Solution by UV/Persulfate Process

Xiangyi Shen ¹, Jing Xu ^{2,*}, Ivan P. Pozdnyakov ^{3,4} and Zizheng Liu ^{5,*} 

¹ Department of Environmental Science, School of Resource and Environmental Sciences, Wuhan University, Wuhan 430079, China; xyshenwhu@outlook.com

² State Key Laboratory of Water Resources and Hydropower Engineering Science, Wuhan University, Wuhan 430072, China

³ Institute of Chemical Kinetics and Combustion, Institutskaya 3, 630090 Novosibirsk, Russia; pozdnyak@kinetics.nsc.ru

⁴ Novosibirsk State University, Pirogova str. 2, 630090 Novosibirsk, Russia

⁵ School of Civil Engineering, Wuhan University, Wuhan 430072, China

* Correspondence: jingxu0506@whu.edu.cn (J.X.); lzz2015@whu.edu.cn (Z.L.)

Received: 26 February 2018; Accepted: 4 April 2018; Published: 13 April 2018



Abstract: Used as a kind of feed additive, *p*-arsanilic acid can pose a potential risk to organisms when abandoned in the environment. The photodegradation of *p*-ASA was investigated under UV-C irradiation in the presence of persulfate (PS) in this work. The addition of PS facilitated the decomposition of *p*-ASA and notably, the presence of 50 mmol PS brought about a nearly complete mineralization after 3 h, while an insignificant total organic carbon (TOC) removal was observed under UV irradiation ($\lambda = 254$ nm) only. Experimental results proved that sulfate radical ($\text{SO}_4\bullet^-$) was responsible for the promotion effect. The cleavage of As-C bond released inorganic arsenic and caused the occurrence of various organic products, for example, hydroxybenzaldehyde, nitrobenzene, benzenediol sulfate, and biphenylarsinic acid. The application of PS with UV-C light may throw a light on thorough treatment for *p*-ASA containing wastewater.

Keywords: *p*-arsanilic acid; photodegradation; UV/persulfate system; sulfate radical

1. Introduction

p-Arsanilic acid (*p*-ASA), a kind of organoarsenic feed additives, are utilized worldwide in order to promote the growth of animals and prevent diseases [1–3]. Though the toxicity of those organoarsenic additives are quite low, disputes about their application still have been aroused in recent years, because of the potential health risks and environmental hazard caused by the residual of arsenicals in livestock products and the discharge of agricultural effluents [3–6]. In fact, organoarsenic additives (including *p*-ASA) might undergo environmental transformation to produce arsenic species of stronger toxicity (i.e., inorganic As(III)) through biological or chemical processes [7–10]. This environmental behavior of *p*-ASA contributes to the elevated level of arsenic around the farms [11,12], posing a high threat to the environment and human health as a consequence. Hence, great attention should be paid to developing effective and low-cost approaches to the treatment of organoarsenic wastewater.

Photochemical degradation plays an important role in transformation of arsenic compounds in aqueous systems and efficient decomposition of *p*-ASA via UV irradiation has been previously reported [13–17]. However, rapid degradation of *p*-ASA during UV irradiation treatment is accompanied with a weak decrease of total organic carbon (TOC) [13–15], an indicator of the severity of organic pollution [18], suggesting a negligible mineralization and the accumulation of aromatic by-products [13,19] with questionable toxicity. Improved photochemical treatments are therefore needed for the *p*-ASA containing agriculture effluents.

Advanced oxidation processes (AOPs) have been successfully applied in the treatment of wastewater, owing to its capability of mineralization and detoxification of many organic pollutants [20–23]. Recently, sulfate radical ($\text{SO}_4^{\bullet-}$) based AOPs have gained much more attention [20,24], among which activated-persulfate (PS) based system is of popularity due to its stability in aqueous solution [21]. PS is generally activated via UV, heat, base, transition metals, ultrasound and some synthetic catalysts [25,26]. Consequently, the applications of PS based system to numerous pollutants have been studied [27], while the treatment for *p*-ASA has not been reported to the best of our knowledge. In this work, photodegradation of *p*-ASA in PS/UV system was studied. Most attention has been paid to determination of intermediate products, degradation pathways, and conditions of complete *p*-ASA mineralization.

2. Materials and Methods

2.1. Chemicals and Reagents

Arsanilic acid (*p*-ASA, purity, 98%) was purchased from Aladdin Industrial Corporation (Shanghai, China). Methanol (HPLC grade) was purchased from Fisher Chemical. All the other reagents were analytical grade and purchased from Sinopharm Chemical Reagent Co., Ltd. Deionized water (JiBaiRui, Wuhan, China) was used for preparation of solutions.

2.2. Photochemical Experiments

Photochemical experiments were conducted in a cylindrical hollow reactor at 293 K, with a total volume of 700 mL at desirable *p*-ASA and PS dosage. UV-C lamp (5 W, $\lambda = 254$ nm) was used as an irradiation source, with an irradiation zone of 1.25 cm wide. Phosphate buffer (PB) was used at a concentration of 20 mmol L⁻¹ to maintain pH 6 during photochemical reaction. Methanol was used as a terminator agent to prevent any possible thermal reactions in irradiated samples prior to consequent analyses, except for the analysis of TOC.

2.3. Analytical Methods

High performance liquid chromatography (HPLC) (Shimadzu Instrument Co. Ltd., Kyoto, Japan, equipped with a 10 ADVP pump, an SPD-10AVP detector, and a Supelco Discovery C18 column, 4.6 × 250 mm, 5 μm) was employed to determine the concentration of *p*-ASA during photolysis as described in previous work [15]. Inorganic arsenic species (As^{III} and As^{V}) were analyzed by hydride generation atomic fluorescence spectrometry (HG-AFS, JiTian Instrument Co. Ltd., Beijing, China), detailed analyzing procedures also have been given in [15]. Total organic carbon (TOC) was analyzed by a Vario TOC analyzer (Elementar, Langensfeld, Germany). The organic by-products were determined by liquid chromatography–mass spectrometry (LC–MS, Agilent Technologies Co. Ltd., Beijing, China) in the positive mode.

3. Results and Discussion

As depicted in Figure 1, >90% of *p*-ASA is photooxidized directly by the irradiation of UV-C light within 30 min, while the addition of 5 mmol L⁻¹ PS caused a noticeable enhancement to the degradation that it took only ~7 min to achieve a complete removal of *p*-ASA. Additionally, the enhancement in photooxidation efficiency strengthened with PS dosage increase. Control experiments showed no obvious change in *p*-ASA concentration under dark conditions, either with or without PS, suggesting the absence of thermal degradation of *p*-ASA by PS.

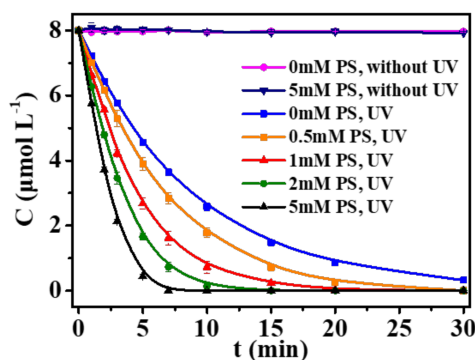


Figure 1. Degradation of *p*-ASA in different systems. Conditions: (*p*-ASA) = 8 $\mu\text{mol L}^{-1}$, (PS) = 1 mmol L^{-1} , (PB) = 20 mmol L^{-1} , pH = 6.

Our previous work [15] showed an insignificant TOC removal of *p*-ASA after UV-C treatment only, while in this work a sharp decrease in TOC was obtained in UV/PS system. As depicted in Figure 2, ~90% TOC elimination was achieved after 180 min irradiation. It was worth to note that only 23% TOC was removed on the stage of *p*-ASA degradation (<45 min of irradiation) with a relatively slow rate, while a faster removal of TOC was gained under UV irradiation for a longer time (>45 min). This fact indicated that TOC removal was mainly connected with the oxidation of by-products. Consequently, a good TOC conversion in UV/PS system implied its potential of industrial application in the treatment for *p*-ASA containing wastewater.

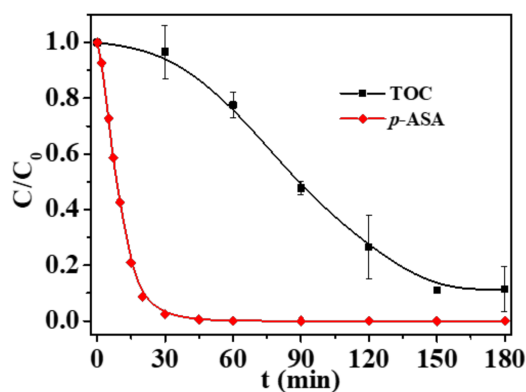


Figure 2. Changes of total organic carbon (TOC) with the degradation of *p*-ASA. Conditions: (*p*-ASA) = 80 $\mu\text{mol L}^{-1}$, (PS) = 50 mmol L^{-1} , (PB) = 20 mmol L^{-1} , pH = 6.

$\text{SO}_4\bullet^-$ has been reported as the dominant radical generated in the process of PS activation in neutral and acid solution [28]. To elucidate more insight of the promotion effect in UV/PS system, ethanol (EtOH) was used as a radical scavenger [29]. The initial reaction rate (calculated in terms of the degradation of *p*-ASA from the first three points during the irradiation) decreased from 1.14 $\mu\text{mol L}^{-1} \text{min}^{-1}$ to 0.49 $\mu\text{mol L}^{-1} \text{min}^{-1}$ in the presence of 40 mmol L^{-1} EtOH (Figure 3) in UV/PS system, confirming the contribution of $\text{SO}_4\bullet^-$. Moreover, the presence of EtOH led to a more retarded degradation of *p*-ASA in UV/PS system than that under UV irradiation only (Figure 3, insert). The stronger inhibiting effect caused by the joint presence of EtOH and PS is caused by competition of PS with *p*-ASA for the light quanta [30]. The remaining *p*-ASA underwent direct photolysis and/or oxidation by $^1\text{O}_2$, which was generated via photosensitization [13].

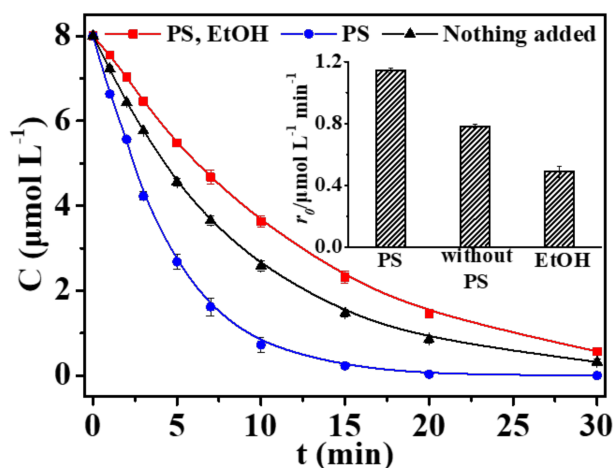


Figure 3. Effect of different quenchers on the degradation of *p*-ASA in UV/PS system. Insert: the initial rate constant of *p*-ASA degradation (r_0) on different conditions. Conditions: (EtOH) = 40 mmol L⁻¹, (*p*-ASA) = 8 μmol L⁻¹, (PS) = 1 mmol L⁻¹, (PB) = 20 mmol L⁻¹, pH = 6.

The generation of $\text{SO}_4\bullet^-$ by activating PS (Equation (1)) [31] is responsible for the TOC decrease, since TOC remains almost invariable in the presence of UV light only [15]. Photoproduct analysis identified the generation of several aromatic compounds: hydroxybenzaldehyde, nitrobenzene, benzenediol sulfate, *o*-ASA (photo-Fries rearrangement product) [15], and biphenylarsinic acid with $[\text{M} + \text{H}]^+$ m/z at 122.9, 123.7, 190.7, 217.7, and 278.9 respectively (Table 1). Previous works [15] reported the cleavage of As-C bond during photolysis, generating aniline at circumneutral conditions, which could be sequentially oxidized to nitrobenzene [21,32,33]. The generation of benzenediol sulfate could result from sulfonation of dihydrobenzene formed both by direct *p*-ASA photolysis [13,14] or its oxidation of by $\text{SO}_4\bullet^-$. Ring-open products—for example, aldehydes and carboxylic acids—with low molecular weight have been reported as the intermediates in AOPs treatment of aromatic compounds [28,32,34]. These products may go through further oxidation to CO_2 or form C-C bond with benzene ring, leading to the generation of aromatic aldehydes/carboxylic acids (like hydroxybenzaldehyde observed in this study) [28,35,36], which explicated the moderate decrease in TOC at the very beginning of irradiation. Liu et al. [37] also proposed aldehydes as one of the possible intermediate products in the oxidation process of benzene by PS in the presence of Fe(III)- and Mn(IV)-containing oxides. However, the obvious cleavage of CO from the primary aldehyde-like products was not observed in our work, followed by the generation of resulting products, probably owing to the more complicated oxidation process caused by the additional involvement of UV light. Phenylarsonic acid [13] was recognized as one of the photoreaction products in the photolysis of *p*-ASA, which could form adducts (for example, biphenylarsonic acid) with aromatic byproducts. Formation of aromatic organoarsenic compounds like biphenylarsonic acid and *o*-ASA could explain the deviation of total arsenics concentrations (As^{T} , the total amount of *p*-ASA, inorganic As^{III} and As^{V}) from initial concentration of *p*-ASA at intermediate stage of the irradiation (Figure 4).



Table 1. The photooxidation products during UV-C irradiation identified by LC-MS.

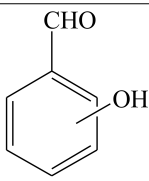
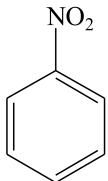
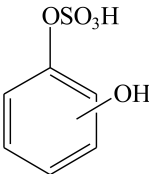
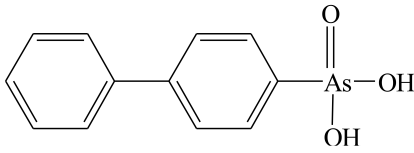
[M + H] ⁺	Structure
122.9	
123.7	
190.7	
278.9	

Figure 4 demonstrated the evolution of arsenic species during *p*-ASA photolysis in PS/UV system. As^{III} was generated as a minor photoproduct at the beginning of the reaction, reaching a plateau at 7 min, at a concentration of 0.36 $\mu\text{mol L}^{-1}$ (<5% of initial *p*-ASA concentration). Concentration of As^{III} was even lower than that in UV system [15] (~10%) due to the presence of oxidative agents (PS and $\text{SO}_4^{\bullet-}$). As^T got a decrease in the first 15 min of irradiation, caused by the generation of newly formed organoarsenicals (biphenylarsinic acid, *o*-ASA). These organic arsenicals could be oxidized by $\text{SO}_4^{\bullet-}$ afterwards, ultimately releasing inorganic arsenic, and as a result, As^T went upward reaching value of 7.7 $\mu\text{mol L}^{-1}$ after the irradiation for 30 min. As^V gained a continuous growth during the photolysis and reached to 7.6 $\mu\text{mol L}^{-1}$ (95% of initial *p*-ASA concentration) at the end of the photoreaction. The equally matched amount of As^V and As^T at the end of the reaction demonstrated a nearly complete transformation from organic arsenic to inorganic As^V.

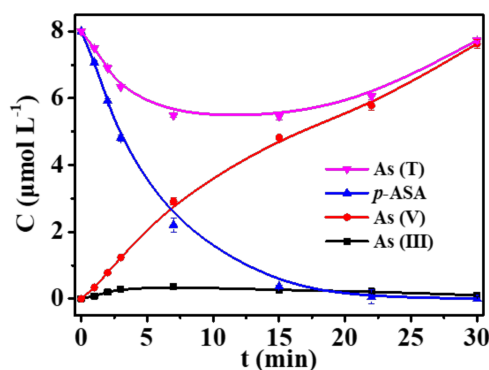


Figure 4. Concentration changes of arsenic species in UV/PS system: (1) As^T (As^{III} + As^V + *p*-ASA); (2) *p*-ASA; (3) As^V; (4) As^{III}. Conditions: (*p*-ASA) = 8 $\mu\text{mol L}^{-1}$, (PS) = 1 mmol L^{-1} , (PB) = 20 mmol L^{-1} , pH = 6.

4. Conclusions

Sulfate radical ($\text{SO}_4^{\bullet-}$), originated from persulfate activated by UV irradiation, was proved to be responsible for the promotion effect and TOC removal at near-neutral pH. In UV/PS system, *p*-ASA ended up with a total conversion to As^{V} , the end product, which can be easily removed from water via many kinds of sorbents. Therefore, the application of persulfate activated by UV ($\lambda = 254 \text{ nm}$) is a promising treatment for *p*-ASA contaminated water.

Acknowledgments: This work was supported by the NSFC-RFBR project 2018, China Postdoctoral Science Foundation (2016M602358), Fundamental Research Funds for the Central Universities (2042017kf0004), and the Russian Foundation for Basic Research (projects 17-03-00252; 18-53-53006_GFEN).

Author Contributions: Jing Xu and Zizheng Liu conceived and designed the experiments; Xiangyi Shen performed the experiments; Jing Xu and Xiangyi Shen analyzed the data; Xiangyi Shen wrote the paper; Ivan P. Pozdnyakov and Zizheng Liu revised the paper.

Conflicts of Interest: The authors declare no conflict of interest.

References

1. Christen, K. Chickens, manure, and arsenic. *Environ. Sci. Technol.* **2001**, *35*, 184A–185A. [[CrossRef](#)] [[PubMed](#)]
2. Liu, X.; Zhang, W.; Hu, Y.; Cheng, H. Extraction and detection of organoarsenic feed additives and common arsenic species in environmental matrices by HPLC-ICP-MS. *Microchem. J.* **2013**, *108*, 38–45. [[CrossRef](#)]
3. Mangalgiri, K.P.; Adak, A.; Blaney, L. Organoarsenicals in poultry litter: Detection, fate, and toxicity. *Environ. Int.* **2015**, *75*, 68–80. [[CrossRef](#)] [[PubMed](#)]
4. Aschbacher, P.W.; Feil, V.J. Fate of [^{14}C]Arsanilic Acid in Pigs and Chickens. *J. Agric. Food Chem.* **1991**, *39*, 146–149. [[CrossRef](#)]
5. Liu, Q.; Peng, H.; Lu, X.; Le, X.C. Enzyme-assisted extraction and liquid chromatography mass spectrometry for the determination of arsenic species in chicken meat. *Anal. Chim. Acta* **2015**, *888*, 1–9. [[CrossRef](#)] [[PubMed](#)]
6. Peng, H.; Hu, B.; Liu, Q.; Yang, Z.; Lu, X.; Huang, R.; Li, X.F.; Zuidhof, M.J.; Le, X.C. Liquid chromatography combined with atomic and molecular mass spectrometry for speciation of arsenic in chicken liver. *J. Chromatogr. A* **2014**, *1370*, 40–49. [[CrossRef](#)] [[PubMed](#)]
7. Stolz, J.F.; Perera, E.; Kilonzo, B.; Kail, B.; Crable, B.; Fisher, E.; Ranganathan, M.; Wormer, L.; Basu, P. Biotransformation of 3-nitro-4-hydroxybenzene arsonic acid (Roxarsone) and release of inorganic arsenic by clostridium species. *Environ. Sci. Technol.* **2007**, *41*, 818–823. [[CrossRef](#)] [[PubMed](#)]
8. Ji, Y.; Shi, Y.; Kong, D.; Lu, J. Degradation of roxarsone in a sulfate radical mediated oxidation process and formation of polynitrated by-products. *RSC Adv.* **2016**, *6*, 82040–82048. [[CrossRef](#)]
9. Garbarino, J.R.; Bednar, A.J.; Rutherford, D.W.; Beyer, R.S.; Wershaw, R.L. Environmental fate of roxarsone in poultry litter. I. Degradation of roxarsone during composting. *Environ. Sci. Technol.* **2003**, *37*, 1509–1514. [[CrossRef](#)] [[PubMed](#)]
10. Bednar, A.J.; Garbarino, J.R.; Ferrer, I.; Rutherford, D.W.; Wershaw, R.L.; Ranville, J.F.; Wildeman, T.R. Photodegradation of roxarsone in poultry litter leachates. *Sci. Total Environ.* **2003**, *302*, 237–245. [[CrossRef](#)]
11. Jones, F.T. A broad view of arsenic. *Poult. Sci.* **2007**, *86*, 2–14. [[CrossRef](#)] [[PubMed](#)]
12. Woolson, E.A. Fate of arsenicals in different environmental substrates. *Environ. Health Perspect.* **1977**, *19*, 73–81. [[CrossRef](#)] [[PubMed](#)]
13. Zhu, X.D.; Wang, Y.J.; Liu, C.; Qin, W.X.; Zhou, D.M. Kinetics, intermediates and acute toxicity of arsanilic acid photolysis. *Chemosphere* **2014**, *107*, 274–281. [[CrossRef](#)] [[PubMed](#)]
14. Xie, X.; Hu, Y.; Cheng, H. Rapid degradation of *p*-arsanilic acid with simultaneous arsenic removal from aqueous solution using Fenton process. *Water Res.* **2016**, *89*, 59–67. [[CrossRef](#)] [[PubMed](#)]
15. Li, S.; Xu, J.; Chen, W.; Yu, Y.; Liu, Z.; Li, J.; Wu, F. Multiple transformation pathways of *p*-arsanilic acid to inorganic arsenic species in water during UV disinfection. *J. Environ. Sci. (China)* **2016**, *47*, 39–48. [[CrossRef](#)] [[PubMed](#)]
16. Czaplicka, M.; Bratek, Ł.; Jaworek, K.; Bonarski, J.; Pawlak, S. Photo-oxidation of *p*-arsanilic acid in acidic solutions: Kinetics and the identification of by-products and reaction pathways. *Chem. Eng. J.* **2014**, *243*, 364–371. [[CrossRef](#)]

17. Czaplicka, M.; Jaworek, K.; Bąk, M. Study of photodegradation and photooxidation of p-arsanilic acid in water solutions at pH = 7: Kinetics and by-products. *Environ. Sci. Pollut. Res.* **2015**, *22*, 16927–16935. [[CrossRef](#)] [[PubMed](#)]
18. Koda, E.; Miszkowska, A.; Sieczka, A. Levels of Organic Pollution Indicators in Groundwater at the Old Landfill and Waste Management Site. *Appl. Sci.* **2017**, *7*, 638. [[CrossRef](#)]
19. Wang, A.; Teng, Y.; Hu, X.; Wu, L.; Huang, Y.; Luo, Y.; Christie, P. Photodegradation of diphenylarsinic acid by UV-C light: Implication for its remediation. *J. Hazard. Mater.* **2016**, *308*, 199–207. [[CrossRef](#)] [[PubMed](#)]
20. Matzek, L.W.; Carter, K.E. Activated persulfate for organic chemical degradation: A review. *Chemosphere* **2016**, *151*, 178–188. [[CrossRef](#)] [[PubMed](#)]
21. Chen, W.S.; Huang, C.P. Mineralization of aniline in aqueous solution by electrochemical activation of persulfate. *Chemosphere* **2015**, *125*, 175–181. [[CrossRef](#)] [[PubMed](#)]
22. Chen, W.S.; Jhou, Y.C.; Huang, C.P. Mineralization of dinitrotoluenes in industrial wastewater by electro-activated persulfate oxidation. *Chem. Eng. J.* **2014**, *252*, 166–172. [[CrossRef](#)]
23. Wang, C.W.; Liang, C. Oxidative degradation of TMAH solution with UV persulfate activation. *Chem. Eng. J.* **2014**, *254*, 472–478. [[CrossRef](#)]
24. Pari, S.; Wang, I.A.; Liu, H.Z.; Wong, B.M. Sulfate radical oxidation of aromatic contaminants: A detailed assessment of density functional theory and high-level quantum chemical methods. *Environ. Sci. Process. Impacts* **2018**, *19*, 395–404. [[CrossRef](#)] [[PubMed](#)]
25. Oh, W.-D.; Dong, Z.; Lim, T.-T. Generation of sulfate radical through heterogeneous catalysis for organic contaminants removal: Current development, challenges and prospects. *Appl. Catal. B Environ.* **2016**, *194*, 169–201. [[CrossRef](#)]
26. Duan, X.; Sun, H.; Kang, J.; Wang, Y.; Indrawirawan, S.; Wang, S. Insights into Heterogeneous Catalysis of Persulfate Activation on Dimensional-Structured Nanocarbons. *ACS Catal.* **2015**, *5*, 4629–4636. [[CrossRef](#)]
27. Huang, W.; Bianco, A.; Brigante, M.; Mailhot, G. UVA-UVB activation of hydrogen peroxide and persulfate for advanced oxidation processes: Efficiency, mechanism and effect of various water constituents. *J. Hazard. Mater.* **2018**, *347*, 279–287. [[CrossRef](#)] [[PubMed](#)]
28. Olmez-Hanci, T.; Arslan-Alaton, I. Comparison of sulfate and hydroxyl radical based advanced oxidation of phenol. *Chem. Eng. J.* **2013**, *224*, 10–16. [[CrossRef](#)]
29. Xu, J.; Ding, W.; Wu, F.; Mailhot, G.; Zhou, D.; Hanna, K. Rapid catalytic oxidation of arsenite to arsenate in an iron(III)/sulfite system under visible light. *Appl. Catal. B Environ.* **2016**, *186*, 56–61. [[CrossRef](#)]
30. Chen, J.; Zhang, P. Photodegradation of perfluorooctanoic acid in water under irradiation of 254 nm and 185 nm light by use of persulfate. *Water Sci. Technol.* **2006**, *54*, 317–325. [[CrossRef](#)] [[PubMed](#)]
31. Gao, Y.Q.; Gao, N.Y.; Deng, Y.; Yang, Y.Q.; Ma, Y. Ultraviolet (UV) light-activated persulfate oxidation of sulfamethazine in water. *Chem. Eng. J.* **2012**, *195–196*, 248–253. [[CrossRef](#)]
32. Xie, X.; Zhang, Y.; Huang, W.; Huang, S. Degradation kinetics and mechanism of aniline by heat-assisted persulfate oxidation. *J. Environ. Sci.* **2012**, *24*, 821–826. [[CrossRef](#)]
33. Zhang, Y.Q.; Xie, X.F.; Huang, W.L.; Huang, S. Degradation of aniline by Fe²⁺-activated persulfate oxidation at ambient temperature. *J. Cent. South Univ.* **2013**, *20*, 1010–1014. [[CrossRef](#)]
34. Zhang, Z.; Xiang, Q.; Glatt, H.; Platt, K.L.; Goldstein, B.D.; Witz, G. Studies on pathways of ring opening of benzene in a Fenton system. *Free Radic. Biol. Med.* **1995**, *18*, 411–419. [[CrossRef](#)]
35. Olmez-Hanci, T.; Arslan-Alaton, I.; Genc, B. Bisphenol A treatment by the hot persulfate process: Oxidation products and acute toxicity. *J. Hazard. Mater.* **2013**, *263*, 283–290. [[CrossRef](#)] [[PubMed](#)]
36. Rodríguez, E.M.; Fernández, G.; Klammerth, N.; Maldonado, M.I.; Álvarez, P.M.; Malato, S. Efficiency of different solar advanced oxidation processes on the oxidation of bisphenol A in water. *Appl. Catal. B Environ.* **2010**, *95*, 228–237. [[CrossRef](#)]
37. Liu, H.Z.; Bruton, T.A.; Li, W.; Buren, J.V.; Prasse, C.; Doyle, F.M.; Sedlak, D.L. Oxidation of benzene by persulfate in the presence of Fe(III)- and Mn(IV)-containing oxides: Stoichiometric efficiency and transformation products. *Environ. Sci. Technol.* **2016**, *50*, 890–898. [[CrossRef](#)] [[PubMed](#)]

